Chapter 6

Sampling in closed loop control systems

Process control is the engineering discipline of causing the variables of a process to conform to some desired values. In many modern control applications one uses the power of digital processing techniques to perform desired control tasks. As was mentioned before in Chapter 1, the majority of systems to be controlled are of analog nature, which implies that A/D- and D/A-conversions are principal operations in digital control systems. In contrast to the situation in signal processing, here the emphasis is not on optimal signal reconstruction, but on appropriate control of processes.

In most digital control systems sampling is carried out by point measurements, with or without pre-filtering, and reconstruction by zero-order hold devices. In the previous chapters we have discussed several alternative sampling schemes, which provide L^2-optimal signal representation. These schemes can be used inside closed-loop control systems, and might improve their overall performance. The central question in this chapter is to determine the effects of alternative filters on this performance.

In Section 6.1, we discuss the signal reconstruction problem in the framework of a digital closed-loop control system. This leads to a number of interesting questions, which form the motivation for the work described in this chapter. Before going into this, we globally review control system analysis and design in Section 6.2. Here we also present an example system which is used in our further investigation, and discuss some specific topics related to digital control. Section 6.3 is devoted to the analysis of a multirate sampled data system (MSDS), i.e., a discrete-time system with multiple sampling frequencies. The problem to be analyzed is formulated in terms of an MSDS. Then we are ready to return to the basic question given above. Control systems with different filters are analyzed in Section 6.4, both by the methods developed in Section 6.3 and by means of computer simulations. Finally, Section 6.5 presents concluding remarks.

6.1 Digital control and optimal signal reconstruction

In this section we discuss the role of optimal signal reconstruction in digital control systems. From this point of view we motivate our experiments to be discussed later in this chapter.

Introduction

A general control system consists of two subsystems: the *plant G*, i.e., the system to be controlled, and the *controller H*, the system that performs the control task. The latter consists in obtaining a satisfactory response to external inputs. In many applications, the goal is to maintain the plant's output *y* to follow the reference input *r*, independent from varying system loads, disturbances and other external effects. Such systems are called input tracking systems.

We consider *closed-loop systems*, in which the output of the plant is fed back to the controller, giving the latter a notion of the effect of its actions. A simple closed-loop control system is depicted in Figure 6.1. It consists of a controller and a plant. The controller drives the plant by the actuating signal *m*. The plant's output *y* is fed back and is combined with an external reference input *r* to the so-called error signal *e*, which serves as input to the controller.

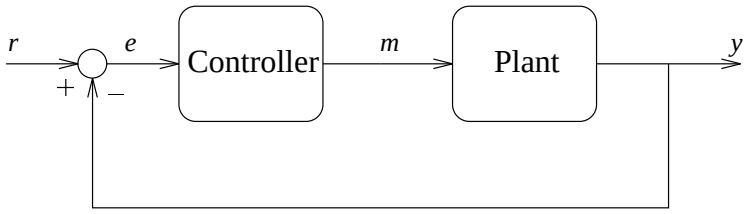

FIGURE 6.1: *A closed-loop control system. Controller and plant are connected into a feedback configuration. We distinguish the following signals: the reference input r, the actuating signal m and the plant's output y.*

Analysis of a control system involves the determination of the system response. This can be carried out experimentally, or by estimating the response on the basis of a system model. Then, it is the task of control system design to achieve a desired overall system response by modifying the controller *H*.

Digital controllers

In digital control systems, the controller operation is implemented digitally. In the majority of control applications, however, the plant is an analog system. Digital control then results in hybrid systems, i.e., systems having both continuous-time and discrete-time parts. Such systems are also referred to as *sampled data systems* (SDS). Here the controller consists of three subsystems: a sampler, a digital controller and a so-called hold device, see Figure 6.2. The hold device converts a discrete-time signal to a continuous-time signal. In other words, it implements a reconstruction operation as defined in Section 2.1. A commonly used hold device is the *zero-order hold* (ZOH), which keeps the output constant at the value of the last input-sample until the next sample becomes available. Other hold devices are mentioned in the literature [FPW90]. For example, the *first-order hold* uses the signal derivative to improve reconstruction.

A drawback of digital control is that *aliasing* may occur. The continuous-time input of a controller may be affected by high-frequency noise components, which turns into low-frequency components after sampling. The controller will base its control strategy upon the disturbed signal and might drive the plant into an undesired state. In many designs, the sampler is preceded by an anti-alias filter to avoid the effects of aliasing.

The scheme in Figure 6.2 shows some resemblance to the general sampling scheme, certainly if the sampler is preceded by an anti-alias filter. Here, an interesting question arises: What happens

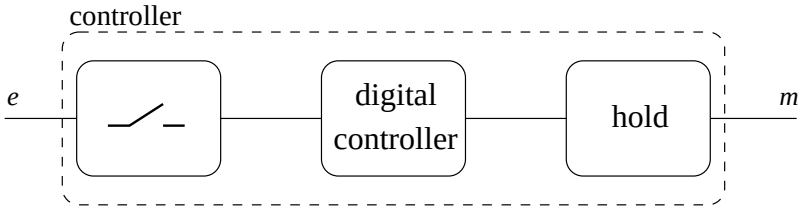

FIGURE 6.2: *The controller in a digital control system, consisting of a sampler, a digital controller, and a hold-device.*

if we embed the digital controller in the general sampling scheme? In particular, does choosing one of the L^2-optimal schemes improve the control system behavior, since the combination of a ZOH and a zero-order B-spline pre-filter without further system modification already reveals an L^2-optimal signal reconstruction?

We expect the behavior to improve. Sampling and reconstruction according to the general sampling scheme with L^2-optimal filter combinations provide an optimal representation of a signal in terms of its samples. Hence, the controller has optimal information about its input and thereby about the state of the plant. It can, therefore, better adapt to the plant's state, which will result in a better control system performance.

Occurrence of delays in a system have destabilizing effects. Inserting filters in the control loop, we also introduce extra delays, since causal filters (see Section 4.5) lead to phase shifts. Note that the non-causal filters discussed in Chapter 5 cannot be used in control systems, because the future values of their inputs, required to evaluate their outputs, are not available. Hence, we have to translate the filter responses in time to make them causal. For example, the B-spline filter of order 1 and down-sampling factor 2 has the following impulse response:

$$h_{-1} = 1/2,\ h_0 = 1,\ h_1 = 1/2.$$

The corresponding causal filter is:

$$h_0 = 1/2,\ h_1 = 1,\ h_2 = 1/2.$$

Note that the first (non-causal) filter does not introduce a phase shift, whereas the second filter does.

Research objectives

Summarizing, we are interested in the effect of inserting alternative filters in the sampling and reconstruction part of digital controllers. These effects seem to go in opposite directions. On the one hand, the filters may have a positive effect on the quality of the signal reconstruction, and on the other hand, the filters may be destabilizing due to the time-delays involved.

More specifically, we pose the following questions:

- How is the overall system behavior affected by insertion of pre- and post-filters?
- Are there indeed positive and negative effects and do they cancel each other?

- Which filter parameters are the most important ones?
- Does an L^2-optimal combination improve system behavior compared to non-optimal combinations?
- Does this modification affect system analysis and design methods?
- What is the answer to the above questions if anti-alias filtering is required?

The literature on control systems is rather vague about the choice of filters in control loops. We are not aware of any thorough analysis. In [FPW90] it is mentioned that the lagging effect of more complex filters does not pay off in terms of enhanced system performance. It seems that the choice of the ZOH is often based on common practice. Concerning anti-alias filters, most references lead to a publication of Corripio et al. [CCP73]. They analyzed the effect of an anti-alias filter on certain performance indices, but only focussed on the first-order lag filter and its digital FIR and IIR approximations. We have not found any study in which both anti-alias filter and reconstruction method (post-filter) were varied.

Therefore, we will analyze a simple control loop with different pre-and post-filters, presented in Figure 6.3. Hereby we attempt to answer the questions stated above. The analysis is carried out for a simple, second-order plant.

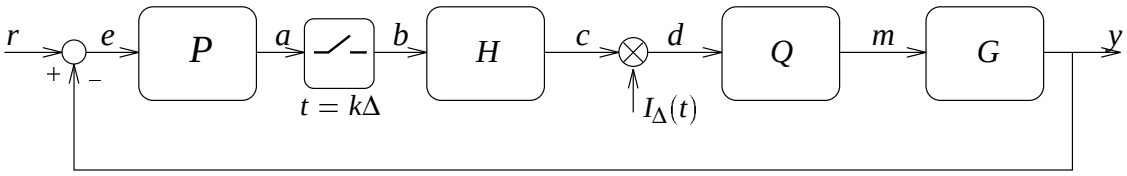

FIGURE 6.3: *A feedback control system. The (digital) controller is embedded in the general sampling scheme. Signals are denoted in lower case, systems in upper case. The different subsystems are pre-filter P, controller H, post-filter Q, and plant G.*

6.2 Review of control system analysis and design

In this section we briefly address analysis and design of control systems. We will illustrate this by means of a simple plant model. For a thorough introduction to control systems we refer to [FPEN94, Ana84].

6.2.1 System modelling

Control systems are often modelled as linear, time-invariant systems. A convenient analysis tool is the Laplace transform. It is used in favor of the Fourier transform, since it is capable of handling one-sided initial value problems (transients) and signals with exponential growth.

The (one-sided) Laplace transform of a signal x is given by

$$X(s) = \int_0^\infty x(t)\, e^{-st}\, \mathrm{d}t,$$

where s is the complex Laplace-variable, $s = \sigma + i\omega$. The Laplace representation of a system (the transfer function $H(s)$) is obtained by Laplace transforming its impulse response h. Hence, for a system H with input x and output y the transfer function is

$$H(s) = \frac{Y(s)}{X(s)} = (Lh)(s),$$

with $X(s)$ the Laplace transform of the input signal, and $Y(s)$ the Laplace transform of the output signal.

The discrete-time equivalent of the Laplace transform is the Z-transform. The (one-sided) Z-transform of a sequence x_k is

$$X(z) = \sum_{0}^{\infty} x_k z^{-k}.$$

Here z is a complex variable: $z = \rho e^{i\omega\Delta}$, and Δ is the sampling interval. Also in the discrete-time case the transfer function of a system $H(z)$ is obtained by transforming its impulse response h_k.

For a discussion on convergence of the transform and for the inversion formulae for both transforms we refer to Appendix A.

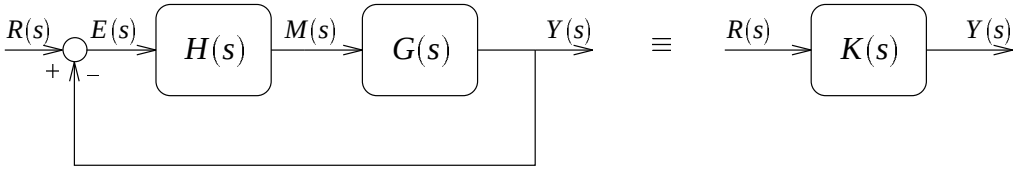

FIGURE 6.4: *A feedback control system and its equivalent system.*

It is possible to calculate the overall transfer function of a system, which is composed of different blocks. The overall transfer function of the closed-loop system in Figure 6.4 can be obtained by block diagram reduction methods. In this case the closed-loop transfer function is

$$\frac{Y(s)}{R(s)} = \frac{G(s)H(s)}{1 + G(s)H(s)} =: K(s). \tag{6.1}$$

It is clear from (6.1) that the overall response $K(s)$ can be altered by modifying the controller $H(s)$.

6.2.2 Response specification

The system response is often specified by certain parameters. We distinguish transient response specification parameters, which describe the response to a transient input (e.g., a step), and the steady state response parameters, which describe the system output after the transient has died out. The most common transient response parameters are illustrated in Figure 6.5.

Another important parameter of control systems is *bandwidth*. Most control systems have a low-pass character. The bandwidth is the frequency at which system output will track a harmonic

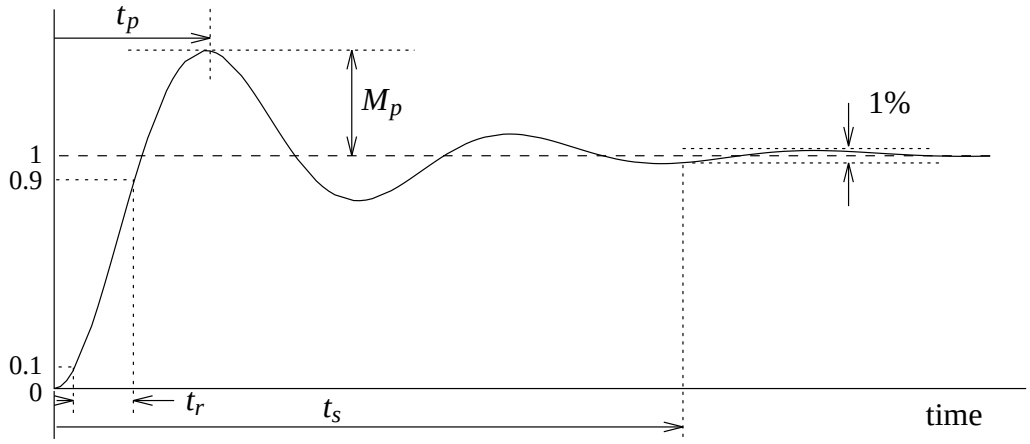

t_r	rise time	time to reach the vicinity of a new set point
t_s	settling time	time after which transient effects have damped out
M_p	overshoot	maximum deviation of system output from its final value
t_p	peak time	time to reach the maximum overshoot point

FIGURE 6.5: *Transient response parameters for step input.*

input in a satisfactory manner. In general, the bandwidth of an overall closed-loop system is quite different from the bandwidth of the plant, depending on the dynamics of the controller.

Other specification methods involve the so-called *performance indices.* These are quantitative measures of system performance. The indices have in common that they provide a measure of the error signal e (cf. Figure 6.1). Commonly used performance indices are listed in Table 6.1. The upper limit of the integrals in commonly set to the settling time t_s. A further important specification parameter is sensitivity to internal parameter variations.

TABLE 6.1: *Performance indices*

Name	Description	Equation
ISE	Integral of Square Error	$\int_0^T e^2(t)\,\mathrm{d}t$
IAE	Integral of Absolute Error	$\int_0^T \lvert e(t)\rvert\,\mathrm{d}t$
ITAE	Integral of Time-multiplied Absolute Error	$\int_0^T t\,\lvert e(t)\rvert\,\mathrm{d}t$
ITSE	Integral of Time-multiplied Square Error	$\int_0^T t\,e^2(t)\,\mathrm{d}t$

6.2.3 System response

The response of a system can be deduced from the system's transfer function. For this, there are several methods, which can be divided into two categories:

- **Frequency domain methods**
  In the frequency domain methods, systems are analyzed for harmonic inputs. System

response can be visualized by Bode diagrams, Nyquist-diagrams or Nicholts charts. The frequency domain methods also work for discrete-time systems.

- ***s*-plane methods**
  In the *s*-plane methods, the system response is obtained from the location of the poles and zeros of the transfer function in the complex *s*-plane. Especially the poles locations determine the major characteristics of system response. A powerful method of this category is the so-called *root-locus* method, which predicts the migration of the closed-loop poles as function of varying system parameter. Discrete-time systems can be analyzed in the *z*-plane by analogous methods.

6.2.4 The example system

Our example plant is a second-order system. It is motivated by a satellite tracking antenna [FPW90, Appendix A]. The transfer function is:

$$G(s) = \frac{4}{s^2 + 2.8\,s}.$$

The system has two poles at $s = -2.8$ and at $s = 0$. The pole at the origin corresponds to pure integration of the input signal. The system is not stable, but can be turned into a stable one by applying feedback control with a proportional controller $H = 1$. The closed-loop transfer function (6.1) then becomes

$$K(s) = \frac{4}{s^2 + 2.8\,s + 4}. \tag{6.2}$$

This closed-loop system has two poles in the left half plane, at $s = -1.4 \pm 1.4283\,i$, which indicates that the system is stable. Its step response is plotted in Figure 6.6.

The transfer function of the general second-order system is commonly written as

$$K(s) = \frac{\omega_n^2}{s^2 + 2\xi\,\omega_n s + \omega_n^2}, \tag{6.3}$$

with ω_n the (undamped) natural frequency, i.e., the frequency at which the system oscillates, and ξ the damping ratio which indicating how fast the oscillations die out: $\xi = 0$ corresponds to no damping. Relating (6.2) to (6.3), we have $\omega_n = 2$ and $\xi = 0.7$. The damping ratio is smaller than 1, which is in agreement with the small overshoot in the step response of Figure 6.6. The bandwidth of the closed-loop system is $\omega_B = 2$ rad/sec.

For second-order systems, some of the response specification parameters are directly related to ω_n and ξ. For our example, the peak time t_p is given by:

$$t_p = \frac{\pi}{\omega_n\sqrt{1-\xi^2}} \simeq 2.20 \text{ sec},$$

and the overshoot M_p by

$$M_p = \exp(-\pi\xi/\sqrt{1-\xi^2}) \simeq 4.59\ \%.$$

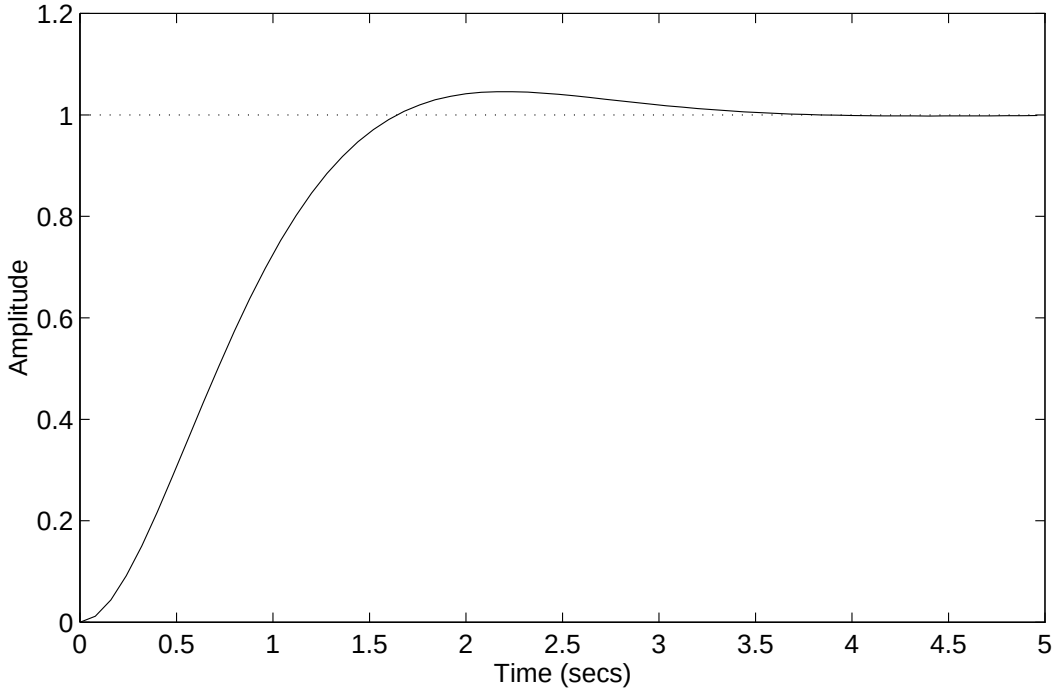

FIGURE 6.6: *The closed-loop step response of the second order system with* $H(s) = 1$ *and* $G(s) = 4/(s^2 + 2.8\,s)$.

6.2.5 Digital control

System analysis and design

Design of a digital control system is complicated due to the fact that systems are hybrid and can, therefore, neither be analyzed by continuous-time methods nor by discrete-time methods. There are two possible strategies (design methods) to overcome this problem [FPW90]:

- **Emulation design**
  Design a continuous-time controller and analyze the system in the continuous domain, using *s*-plane or frequency domain methods. If the design is satisfactory, 'discretize' the controller, i.e., find a discrete-time controller, such that the overall system preserves its characteristics.

- **Discrete design**
  Discretize the plant. Now the whole system is discrete-time. Analysis and design can then be carried out in the *discrete-time domain*, using *z*-plane or frequency domain methods.

Both methods have in common that continuous-time parts of sampled data systems have to be discretized, for which several methods exist [FPW90, Chapter 3].

Sampling rate selection

Selection of sampling rates is an important issue. For economical reasons, sampling rates are kept as low as possible: A lower rate means that there is more time available for control al-

gorithm execution, which can thereby be carried out on slower computers. Digitizing well behaved analog control systems can heavily affect system response. If sampling frequencies is too low, the systems may even become unstable. According to the Nyquist criterion, the sampling frequency should at least be twice as high as the bandwidth of the error signal. This bandwidth is bounded by the system bandwidth, hence $\omega_s \geq 2\,\omega_B$. However, in order to guarantee satisfactory response, a factor of 10 to 20 may be required [FPW90, Ch. 10].

Aliasing and pre-filtering

It was already mentioned that aliasing can have a dramatic effect on system performance. Introduction of anti-alias filters is the answer to this problem. The drawback is that such filters' phase lag affects the overall system behavior.

A commonly used type of filter is a first order low-pass filter, or first-order lag filter (FOL), with transfer function:

$$H(s) = \frac{\omega_f}{s + \omega_f},$$

where ω_f is the cut-off frequency of the filter. A Bode diagram of this filter response for $\omega_f = 1$ is given in Figure 6.7. For values below ω_f, the response is flat, beyond ω_f the slope is -20 dB per decade. The attenuation at ω_f is -3 dB. The cut-off frequency is chosen in such a way that the suppression at the Nyquist frequency $(\omega_s/2)$ is sufficiently high. For example, for a suppression of 90% (-20 dB) at $\omega_s/2$, we obtain the requirement $\omega_s = 20\,\omega_f$. On the other hand, the cut-off frequency must exceed the system's bandwidth, otherwise frequencies that occur naturally in the system will be suppressed as well. As long as both ω_s and ω_f are sufficiently higher than the closed-loop bandwidth ω_B, the effects of the extra phase lag is relatively small and the anti-alias filter can be ignored in the design procedure. This yields a lower limit on the sampling rate, being 20 to 100 times the closed-loop bandwidth ω_B [FPW90].

If ω_f is chosen closer to the bandwidth, the system response will be affected by the extra phase lag. Then the filter characteristics must be taken into account during the design procedure, leading to a more complex design. The cut-off frequency can now be chosen equal to the system bandwidth, allowing sample rates of 5 to 10 times the closed-loop bandwidth [FPW90].

According to the question what suppression is sufficient, the opinions differ. Franklin et al. [FPW90] suggest that ω_s is 5 to 10 times ω_f, yielding a suppression of -8 to -14 dB at the Nyquist frequency. Corripio et al. [CCP73] suggest a value of π times ω_f, corresponding to -5.4 dB.

Zero-order hold

It was already mentioned that the ZOH is a widely used reconstruction operator. Therefore it will be investigated in more detail here.

We define the ZOH to be a hybrid system with discrete-time input and continuous-time output[1]. The response of the ZOH to a discrete-time impulse is

$$h(t) = \begin{cases} 1 & 0 \leq t < \Delta \\ 0 & \text{elsewhere} \end{cases}$$

[1] In many textbooks, the ZOH is defined as a linear, time-invariant system with a rectangular impulse response. In other words, (6.4) is used as characterization of the ZOH.

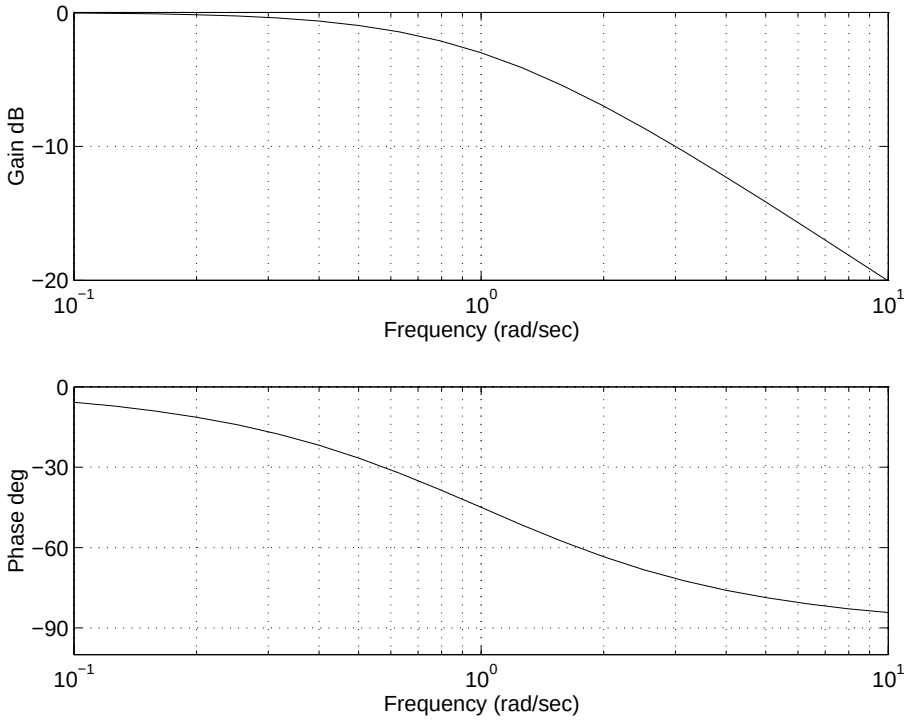

FIGURE 6.7: *Bode diagram of the first-order low-pass filter with $\omega_f = 1$ rad/sec.*

Hence, the ZOH is functionally equivalent to δ-modulation of the input signal, followed by a causal B-spline filter of order zero: $\beta^0 = \chi_{[0,1)}$. The same composite operation is present in the reconstruction part of the general sampling scheme. The Laplace transform of this filter action can be easily derived: the impulse response can be decomposed as a step at $t = 0$ followed by a negative step at $t = \Delta$. This corresponds to:

$$H(s) = \frac{1 - e^{-s\Delta}}{s}. \tag{6.4}$$

The corresponding magnitude response is

$$|H(i\omega)| = \Delta \left| \frac{\sin\, \omega\Delta/2}{\omega\Delta/2} \right|,$$

and the phase is

$$\angle H(i\omega) = -\frac{\omega\Delta}{2}.$$

The Bode diagram is given in Figure 6.8. We conclude that the ZOH acts as a low-pass filter. The attenuation at the Nyquist frequency $\omega = \pi/\Delta$ is -3.9 dB. Note that the filter's response (6.4) is completely determined by the sampling interval Δ.

The composition of sampling and reconstruction by a ZOH introduces a delay. The output of the ZOH is a staircase-like signal, which, on average, lags $\Delta/2$ behind compared to the continuous-time input. This is illustrated in Figure 6.9.

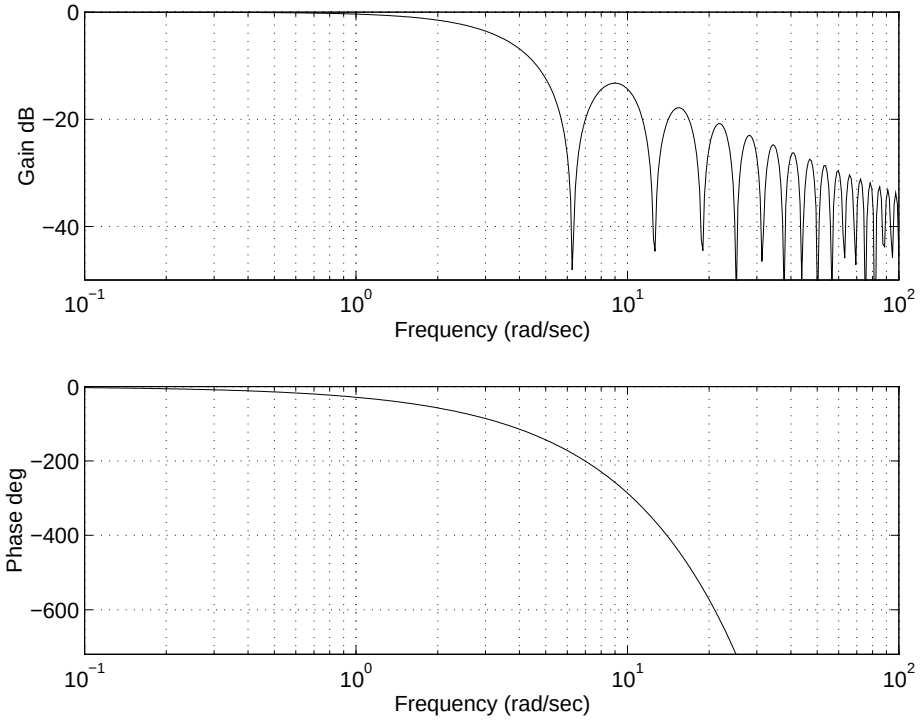

FIGURE 6.8: *Bode diagram of the ZOH filter.* $\Delta = 1 \Leftrightarrow \omega_S = 2\pi$.

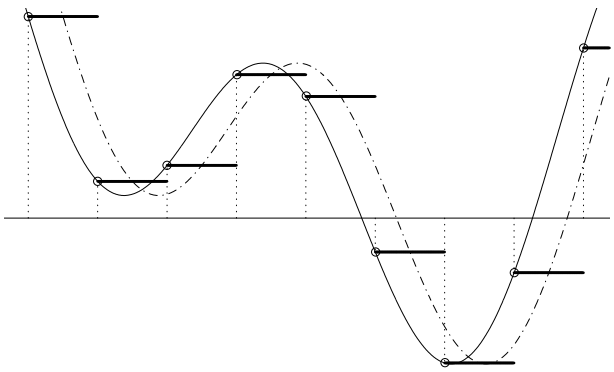

FIGURE 6.9: *The delay introduced by a ZOH. The solid curve is the continuous-time signal. The tiny circles give the sample points (at distance* Δ*) and the horizontal lines the output of the ZOH. The dash-dotted line is a smooth line drawn through the ZOH-output. The net delay is* $\Delta/2$.

6.3 Analysis of multi-rate sampled data control systems

Our goal was to analyze the closed-loop system of Figure 6.3. For this purpose, it is interesting to obtain the overall transfer function. However, due to the fact that sampler and δ-modulator are *time-variant systems,* an overall transfer function does not exist in the general case. A structured method for analysis of systems containing samplers inside the loop is given in [FPW90, Sc. 4.5.].

In order to stay close to our simulation results, we prefer an analysis of the system's discrete-time equivalent. In analogy to Chapter 5 we introduce two sampling rates: a fast rate for reliable simulation of the time-continuous parts and a slow one for the controller. The system then becomes a multirate sampled data system (MSDS). To facilitate the analysis, the higher rate is chosen to be an integer multiple of the lower one, allowing conversion by up- and down-sampling.

Discretization of the whole system of Figure 6.3 yields the discrete equivalent, shown in Figure 6.10. The plant G, and the pre- and post-filters P, Q are discrete-time systems, operating at the fast rate. The controller H operates on the slow rate. Sampling rate conversion is carried out by the up- and down-sampler. The ratio between the two sampling rates is an integer M. All continuous-time parts of Figure 6.3 can be discretized using one of the available discretization methods [FPW90]. Since we assume a fast sampling rate, the error of this process will be small.

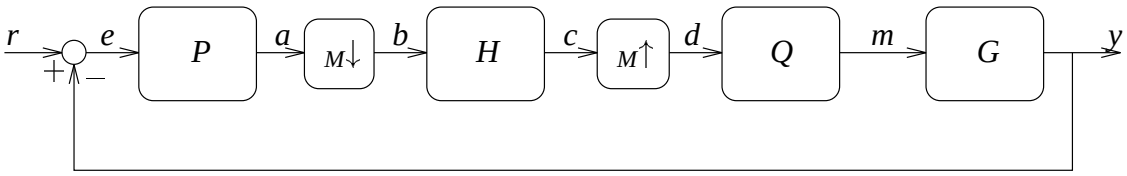

FIGURE 6.10: *A feedback control system with the general sub-sampling scheme. Signals are denoted in lower case, systems in upper case. The different subsystems are pre-filter P, controller H, post-filter Q, and plant G.*

The analysis of an MSDS is still complicated due to the fact that down-sampling is a time-varying operation. This also implies that the overall transfer function does not exist in all cases. In the literature, there is hardly any reference to the analysis of an MSDS. In [FR58], a method is given, but it switches forth and back between the z-domain and the time domain. Here, we derive an input-output relation in terms of Z-transforms. The analysis is fully carried out in the z-domain. Our analysis of MSDS can be regarded as the discrete-time counterpart to the analysis of sampled data systems in [FPW90, Sc. 4.5.].

Up/down sampling

The two principal operations in an MSDS are up-sampling and down-sampling. The up-sampler (see (4.23), p. 60) is characterized by the following relation between the Z-transforms of its input x and its output y:

$$Y(z) := X(z^M), \tag{6.5}$$

where M is the up-sampling factor. Note that this relation cannot be represented in terms of a transfer function.

The corresponding relation for the down-sampler (see (4.24), p. 60) is more complicated:

$$Y(z) = \frac{1}{M}\sum_{k=0}^{M-1} X(e^{\frac{-2ik\pi}{M}} z^{\frac{1}{M}}), \tag{6.6}$$

but for the case $M = 2$ the relation reduces to

$$Y(z) = \frac{X(-\sqrt{z}) + X(\sqrt{z})}{2}.$$

It is easily verified that up-sampling followed by down-sampling is the identity. The composition of down-sampling and up-sampling (discrete δ-modulation, see Section 5.2) becomes

$$Y(z) = \frac{1}{M}\sum_{k=0}^{M-1} X(e^{\frac{-2ik\pi}{M}} z),$$

and, for $M = 2$, reduces to:

$$Y(z) = \tfrac{1}{2}\left(X(z) + X(-z)\right).$$

Discrete δ-modulation can be interpreted as an operator on Z-transforms. We will denote this operator as

$$_M\!\uparrow\!\downarrow : \; X(z) \to Y(z) : \; Y(z) = \frac{1}{M}\sum_{k=0}^{M-1} X(e^{\frac{-2ik\pi}{M}} z). \tag{6.7}$$

Controller position

In our case, the controller is embedded between the down-sampler and the up-sampler. According to relation (5.8) on p. 88, the controller and the up-sampler can be interchanged, but the transfer function of the controller then becomes $H(z^2)$, see Figure 6.11.

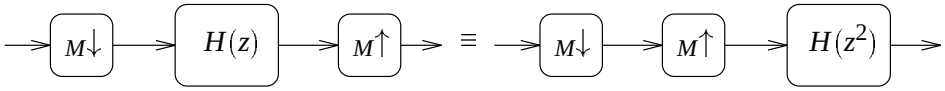

FIGURE 6.11: *Changing the position of the controller (see text).*

Overall system

Let us turn back to the closed loop MSDS in Figure 6.10. We derive the input-output relation for the case $M = 2$. By inspection, we obtain the following equations:

$$\begin{aligned} Y(z) &= G(z)\,Q(z)\,C(z^2) && (6.8)\\ C(z) &= H(z)\,B(z) && (6.9)\\ B(z^2) &= \tfrac{1}{2}\left(A(z) + A(-z)\right) && (6.10)\\ A(z) &= P(z)\,E(z) && (6.11)\\ E(z) &= R(z) - Y(z) && (6.12) \end{aligned}$$

To simplify notation, we introduce the following abbreviations:

$$A := A(z), \qquad A^- := A(-z), \qquad A^2 := A(z^2).$$

Solving for C gives:

$$\begin{aligned} C^2 &= H^2 B^2 \\ &= \tfrac{1}{2}H^2\{A + A^-\} \\ &= \tfrac{1}{2}H^2\{PE + P^-E^-\} \\ &= \tfrac{1}{2}H^2\{PR - PY + P^-R^- - P^-Y^-\}. \end{aligned}$$

Noting that

$$Y(-z) = G(-z)\,Q(-z)\,C(z^2),$$

we obtain

$$C^2 = \tfrac{1}{2}H^2\left\{PR - PGQC^2 + P^-R^- - P^-G^-Q^-C^2\right\} \Leftrightarrow$$

$$C^2\left\{1 + \tfrac{1}{2}H^2(PGQ + P^-G^-Q^-)\right\} = \tfrac{1}{2}H^2(PR + P^-R^-) \Leftrightarrow$$

$$C^2 = \frac{\frac{1}{2}H^2(PR + P^-R^-)}{1 + \frac{1}{2}H^2(PGQ + P^-G^-Q^-)}\,. \tag{6.13}$$

Substituting (6.13) in (6.8) yields

$$Y = \frac{\frac{1}{2}H^2GQ(PR + P^-R^-)}{1 + \frac{1}{2}H^2(PGQ + P^-G^-Q^-)}\,.$$

This can be interpreted as a transfer function $K(z)$ from the filtered and δ-modulated reference signal r to the output y:

$$Y(z) = K(z)\,\tfrac{1}{2}\,[P(z)\,R(z) + P(-z)\,R(-z)]$$

with

$$K(z) = \frac{H(z^2)\,G(z)\,Q(z)}{1 + \frac{1}{2}H(z^2)\,\left[P(z)\,G(z)\,Q(z) + P(-z)\,G(-z)\,Q(-z)\right]}\,. \tag{6.14}$$

Using this transfer function $K(z)$, the system of Figure 6.10 simplifies to the system of Figure 6.12.

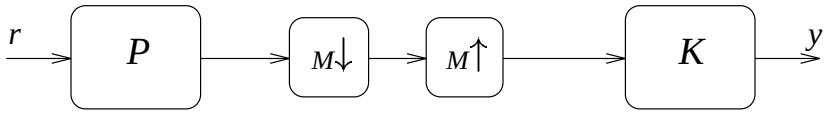

FIGURE 6.12: *The loop-free equivalent of the system in Figure 6.10.*

Using the discrete δ-modulation operator (6.7), this result can be generalized for down-sampling factor M:

$$K(z) := \frac{Y(z)}{{}_M\!\uparrow\!\downarrow\{P(z)\,R(z)\}} = \frac{H(z^2)\,G(z)\,Q(z)}{1 + H(z^2)\,{}_M\!\uparrow\!\downarrow\{P(z)\,G(z)\,Q(z)\}}\,. \tag{6.15}$$

We do not present the proof here, because the case $M = 2$ is illustrative for the general case.

Let us resume. The system of Figure 6.10 is a discrete-time system and can be simulated directly. It does not have a transfer function, though it can be simplified to a system without a loop. This equivalent system (Figure 6.12) can be simulated instead. It has, moreover, a subsystem with transfer function $K(z)$. The time response of this part can be directly estimated from the position of the poles and zeros in the z-plane.

6.4 Analysis of MSDS's with alternative filters

After our discussion of some general topics related to control systems and the presentation of the analysis method for MSDS systems, we are now prepared to return to the original problem: What is the effect of alternative filters in the closed-loop MSDS in Figure 6.10?

In Section 6.4.1, we concentrate on the loop-free equivalent system in Figure 6.12, and further investigate the transfer function $K(z)$ for varying down-sampling factors and different filters. Then we consider the original closed-loop MSDS system, and run simulations under different conditions. The experimental setup is discussed in Section 6.4.2. The results are presented in Section 6.4.3. Both the MSDS analysis and the experiments in this section were carried out to obtain answers to the questions raised at the beginning of this chapter, in Section 6.1. Therefore, we will present the conclusions drawn from this work in the final section of this chapter: Section 6.5.

6.4.1 Analysis of the transfer function $K(z)$

In Section 6.3 we discussed the analysis of a Multirate Sampled Data System. We found that the closed-loop system in Figure 6.10 is equivalent to the loop-free system in Figure 6.12. This result suggests that at least part of the characteristics of the overall system is hidden in the transfer function $K(z)$, defined in (6.15). To study this further, we concentrate on two questions:

- What are the characteristics of $K(z)$ for various down-sampling factors, using the 'standard' situation of no pre-filter and ZOH reconstruction?
- What is the effect of the different filters on $K(z)$?

Regarding the first question, we expect that the response of the original system in Figure 6.10 becomes worse with increasing M and, finally, the system turns unstable. This is motivated by the simple fact that the information reaching the controller reduces and is further delayed when the down-sampling factor M increases. This would imply that the transfer function $K(z)$ must also become unstable. Regarding the second question we have no expectations about the result.

Calculation of $K(z)$

The calculations were carried out for the Z-transform of the general second-order plant :

$$G(z) = \frac{a\,z + b}{z^2 + c\,z + d}.$$

The resulting expression for $K(z)$ was generated by MATHEMATICA[2], using the program listed in Appendix B. It appears that these calculations become quite lengthy for $M = 4$ and even do not terminate for $M \geq 8$.

[2]Copyright 1988-94 Wolfram Research, Inc.

To keep the calculations as simple as possible, we restricted ourselves to B-spline filters of order 0, 1, and 2. The Z-transform of the (discrete-time) B-spline filter of order zero and down-sampling factor M is given by

$$B_M^0(z) = 1 + z^{-1} + \cdots z^{-M+1} = \frac{z^{M-1} + z^{M-2} + \cdots + 1}{z^{M-1}}.$$

The Z-transforms of the higher order splines are obtained by [AU93]

$$B_M^n(z) = \left(B_M^0(z)\right)^{n+1} B_1^n(z),$$

where $B_1^n(z)$ is the Z-transform of the sequence obtained by sampling the causal B-spline at the integers. Note that this relation can be interpreted as the discrete-time counterpart of the recursive relation (4.55) on p. 76.

Further down-sampling in the loop

To present the results for the second-order system, we start with a discrete-time plant, obtained by discretization of the continuous-time plant $G(s) = 4/(s^2 + 2.8\,s)$ using the *matched pole-zero method* and sampling rate $\Delta = 0.8$. The resulting Z-transform is

$$G(z) = \frac{0.5284z + 0.5284}{z^2 - 1.106z + 0.1065}.$$

Since the closed-loop system bandwidth ω_B was equal to 2 rad/sec, the sampling rate is around the Nyquist rate ($\pi/0.8 \simeq 3.92 \simeq 2\,\omega_B$), but significantly less than the required 10 to 20 times ω_B. We therefore expect that further down-sampling will cause the system to become unstable.

TABLE 6.2: *Number of zeros and poles of $K(z)$.*

M	# Zeros	# Poles
1	1	2
2	4	5
4	10	11

The number of zeros and Poles, representing the polynomial orders of the numerator and the denominator of $K(z)$, are given in Table 6.2 for $M = 1,\ 2$, and 4, respectively. Maps of the z-plane are given in Figure 6.13. For $M = 4$, the two poles on the positive real axis are compensated by zeros. These pairs represent common factors in the numerator and the denominator of $K(z)$, which were not removed by MATHEMATICA. The numbers in Table 6.2 are corrected for this.

The resulting $K(z)$ for $M = 1$ equals the closed-loop transfer function with unity feedback $G(z)/(1 + G(z))$. This function corresponds to a stable response. For $M = 2$, the poles are close to the unit circle, corresponding to more oscillation in the response. Finally for $M = 4$, some of the poles are outside the unit circle, which gives an unstable response.

Does a stable/unstable $K(z)$ imply that the overall system of Figure 6.12 is stable/unstable? Suppose $K(z)$ is unstable. Then it is most likely that there is an input r which yields an unstable

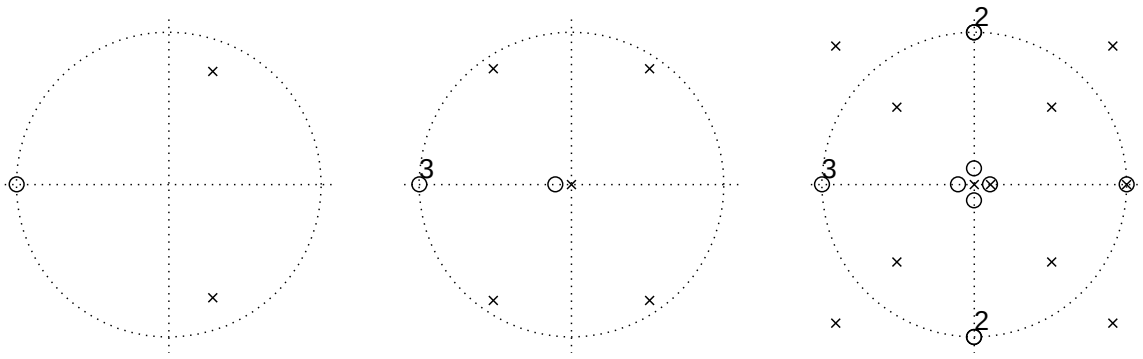

FIGURE 6.13: *Pole-zero maps of $K(z)$.* **Left***: $M = 1$ (no down-sampling),* **middle***: $M = 2$,* **right***: $M = 4$. The poles and zeros are denoted by $\times$ and $\circ$, respectively. The numbers in the figures denote the multiplicity of multiple zeros. The horizontal axis is the real axis, the vertical axis is the imaginary axis. The circle in each map refers to the unit-circle $|z| = 1$.*

response. Hence, the overall system is most likely unstable. On the other hand, if $K(z)$ is stable, the overall system will be stable as well, because the composition of pre-filter, down-sampler and up-sampler always has a bounded response to a bounded input. Hence, the input of $K(z)$ is always bounded and, together with the stability of $K(z)$, the overall system is stable.

Different pre- and post-filters

The transfer functions $K(z)$ were calculated for a number of of B-spline filter combinations, including the l^2-optimal combination of B_0-splines. The pairs are listed in Table 6.3, together with the number of poles and zeros of the resulting $K(z)$. Again, the table is corrected for common factors in numerator and denominator. The pole/zero maps are given in Figure 6.14. Cancelling pole/zero pairs have been removed from the figure.

TABLE 6.3: *Filter pairs and number of zeros and poles of $K(z)$.*

Code	Pre-filter	Post-filter	# Zeros	# Poles
NZ	none	B_0-spline	4	5
NF	none	B_1-spline	5	6
NB	none	B_2-spline	6	7
ZZ	B_0-spline	B_0-spline	5	6
ZF	B_0-spline	B_1-spline	5	6
ZB	B_0-spline	B_2-spline	7	8
FF	B_1-spline	B_1-spline	7	8

Clearly, the combination 'NZ' has the least complex pole-zero map. The corresponding response is close to the response of the continuous-time system. The other filter combinations introduce additional poles/zeros, and all yield responses with larger overshoots and longer oscillations.

Having a closer look at the map for 'ZZ' and the map for 'NF', we see two differences: First, 'ZZ' has a zero at the origin, which is not present for 'NF'. Secondly, 'NF' has an extra zero

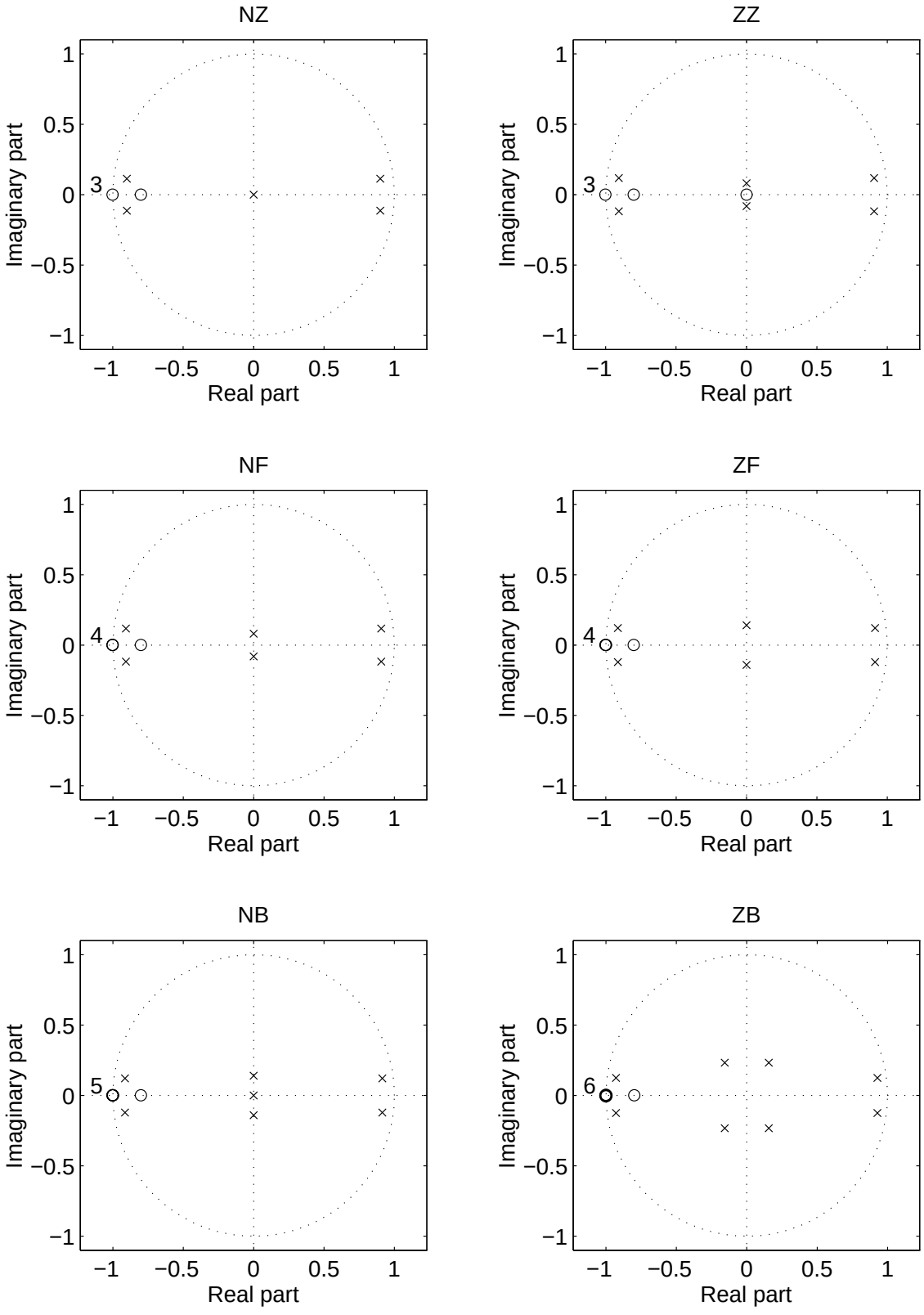

FIGURE 6.14: *Pole-zero maps of $K(z)$. $M = 2$. Different filters. Cancelling pole/zero pairs have been removed. The numbers in the figures denote the multiplicity of multiple zeros.*

at -1. These differences suggest that the transfer function $K(z)$ for 'NF' is obtained from that of 'ZZ' using a system with a pole at the origin and a zero at -1, which corresponds exactly to the zero-order B-spline $B_2^0(z)$. At second sight, this is not surprising, because the term ${}_M\uparrow\downarrow\{P(z)\,G(z)\,Q(z)\}$ in (6.15) is the same for both filter combinations. Since the B_0-spline filter acts as a low-pass filter, we expect the response of the 'NF' combination to be smoother than the 'ZZ' combination.

Compared to the combination 'NZ', the l^2-optimal combination 'ZZ' has a more complex map with poles closer to the unit circle. It seems that the negative effect of extra delay is not compensated by a positive effect due to the better signal reconstruction.

From the pole-zero maps we conclude that the 'NZ' combination corresponds to the best response. However, the transfer function K only partly determines the response of the system in Figure 6.12. To obtain the overall response, simulations were carried out, which will be discussed in the next sections.

6.4.2 Experimental setup

The main goal of our experiments was outlined in the introduction of this chapter: we want to know the effects of alternative filters in multirate sampled data systems.

MATLAB is used as the simulation environment. Its CONTROL TOOLBOX offers functions for control system analysis and design, and simulation tools for obtaining step and other responses. However, MATLAB is not capable to simulate systems with a feedback path, like the system of Figure 6.10. In this case, a step-by-step simulation has to be implemented, which is considerably slower than MATLAB's vectorized approach. Therefore, we are interested whether we can use the loop-free equivalent in Figure 6.12 for our simulation.

Then we compare the performance of the different filters pairs, listed in Table 6.3. The performance is compared in terms of the time-domain specification parameters and the performance indices of Table 6.1, both discussed in Section 6.2.2. The filter combination 'NZ' is used as reference, since this pair represents the standard configuration in digital control. Impulse, step and ramp signals will be used as input signals (reference input r).

So far, comparison with a standard anti-alias filter is not included. For this we restrict ourselves to the zero-order B-spline pre-filter, because the 'ZZ' combination has the lowest phase lag, and this filter is easy to implement (see Chapter 7). We compare the 'ZZ' combination to the standard first-order low-pass filter, subsequently denoted as FOL (First-Order Lag).

It was mentioned before that the cut-off frequency of the FOL is chosen in such a way that the suppression at the Nyquist frequency is sufficiently high. Since there are different opinions of what is considered to be 'sufficiently high', we choose a number of FOL filters with different cut-off frequencies, varying from $\omega_f = \omega_s/2$ to $\omega_f = \omega_s/20$.

In this comparison, we will follow an engineering design procedure, involving the following steps:

- use one of the specification parameters, e.g., the maximum overshoot M_p, as a design goal,

- design a control system satisfying the requirements,
- apply the filters,
- correct the degradation of performance with respect to the particular parameter, and
- evaluate the effect of the resulting design on other parameters.

The sampling interval is kept fixed at $\Delta = 0.08$ which is in agreement with the rule of thumb $\omega_s \simeq 40\,\omega_B$. We compare the system response in terms of the time-domain specification parameters and the performance indices. Then, with white noise added to the feedback path, we measure the noise variance at the plant's output for zero input. This measurement gives information about the anti-aliasing performance of the different filters.

6.4.3 Results

Comparison of the two simulation methods

We have proven the equivalence of the systems in Figures 6.10 and 6.12. Simulations of those two systems should give the same results. This is confirmed by the experiments. However, since the transfer function $K(z)$ contains high powers of z, the system in Figure 6.12 is more sensitive to quantization errors than the system in Figure 6.10. Moreover, noise can only be added to the feedback signal if this signal is actually present. For this reasons we used the step-by-step method for the remaining simulations.

Responses for different filter combinations

The performance of the different filters is given in Table 6.4. The step response and the response to a sine input are depicted in Figures 6.15 and 6.16, respectively. In addition, we generated Bode diagrams and graphs of the impulse responses (both are not included here). We made the following observations:

- The most dominant effect of inserting filters in the control loop is a phase lag, which is apparent from Figure 6.16. From the fact that the combinations 'ZZ' and 'NF' as well as the combinations 'ZF', 'FZ', and 'NB' have a similar phase lag, we conclude that the lag is mainly determined by the sum of the filter lengths of the pre- and the post-filter.
- From Table 6.4, we conclude that the standard configuration 'NZ' has the best values for all parameters, except for the rise-time which decreases for longer filters.
- The damping ratio diminishes with growing filter degree. This results in increasing amplitude of oscillations, and larger settling time. Again, the combinations with the same total length yield a similar response.
- The phase margin PM (relative degree of stability) diminishes with growing filter degree: the system tends to instability.
- The impulse response of the combinations with a pre-filter (ZZ, ZF, ZB) is considerable smaller than that of the combinations without a pre-filter (NZ, NF, NB). Hence, pre-filtering diminishes the system's sensitivity to spikes.

TABLE 6.4: *Response of the closed-loop system with different filter combinations.* $M = 32$

Code	Pre-filter	Post-filter	t_r	M_p	t_s	IAE	ISE	ITAE	ITSE
NZ	—	BSP0	0.9400	0.0863	3.1900	0.8059	0.5173	0.5200	0.1799
NF	—	BSP1	0.8700	0.1404	4.5750	0.9336	0.5914	0.7485	0.2337
NB	—	BSP2	0.8150	0.2105	4.8400	1.1028	0.6841	1.0841	0.3255
ZZ	BSP0	BSP0	0.8700	0.1408	4.6500	1.0120	0.6702	0.8243	0.2829
ZF	BSP0	BSP1	0.8150	0.2087	4.9100	1.1755	0.7598	1.1608	0.3784
ZB	BSP0	BSP2	0.7750	0.2903	5.0950	1.3904	0.8748	1.6678	0.5387
FZ	BSP1	BSP0	0.8200	0.2074	4.9150	1.1725	0.7562	1.1572	0.3761

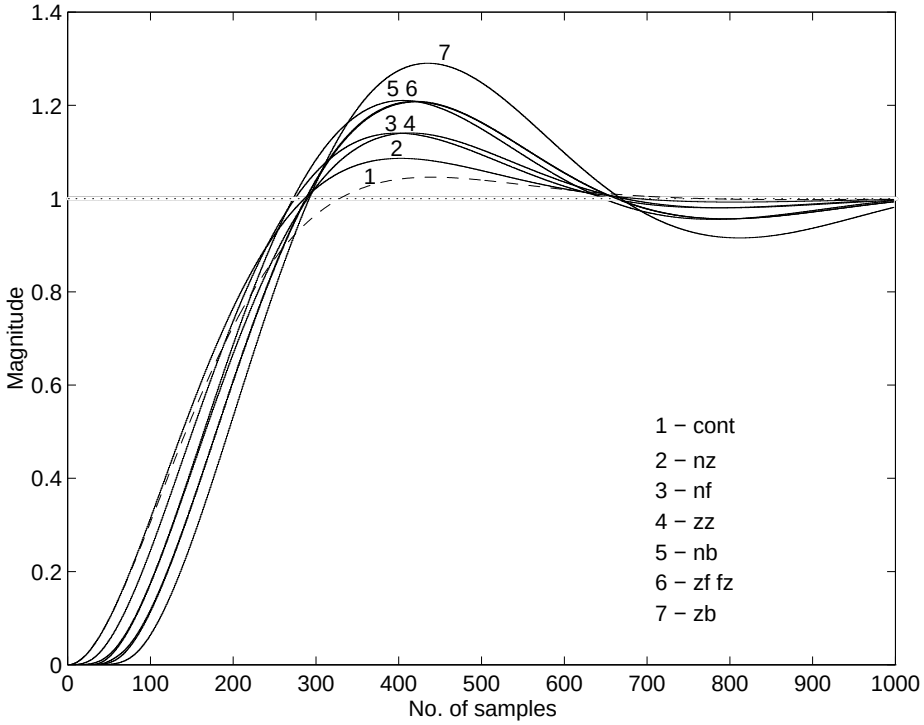

FIGURE 6.15: *Simulated step responses.*

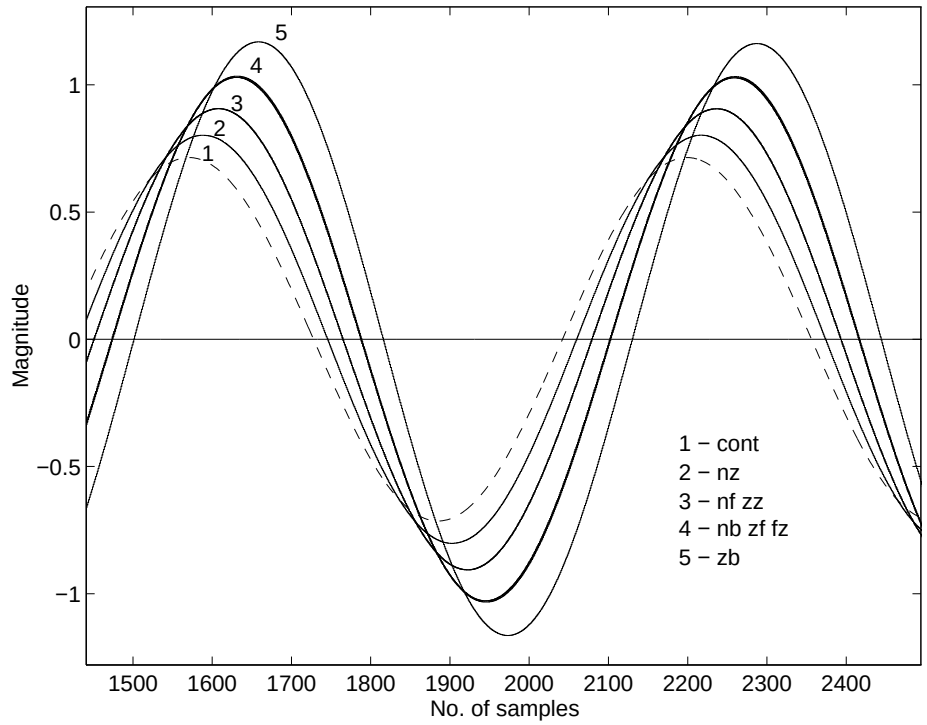

FIGURE 6.16: *Simulated responses to a harmonic input.*

Comparison between B_0-spline and FOL filters

Here, we discuss the comparison between the B_0-spline and the FOL filters, using our procedure as described in the previous section. Different pre-filters were considered and summarized in Table 6.5. The table also contains the attenuation of the different filters at the Nyquist frequency $\omega_s/2$ and at the sample frequency ω_s itself. Frequencies in the interval between them give rise to aliasing and must, therefore, be attenuated by the pre-filter. Attenuation values were obtained from theoretical frequency-magnitude curves.

TABLE 6.5: *The different pre-filters that have been studied.*

#	Type	ω_s/ω_f	Attenuation at $\omega_s/2$ (dB)	Attenuation at ω_s (dB)
a	FOL	2	-3.0	-7.0
b	FOL	π	-5.4	-10.3
c	FOL	5	-8.6	-14.1
d	FOL	10	-14.1	-20.0
e	FOL	20	-20.0	-26.0
f	FOL	40	-26.0	-32.0
z	B_0-spline	–	-3.9	$-\infty$

The systems were designed to have a maximum overshoot of 4.59%. After the filters were inserted in the loop, the overshoot increased in all cases (which is in agreement with the previous experiments). This was compensated by means of a controller gain reduction. The response parameters of the resulting systems are given in Table 6.6. As a consequence of the design

TABLE 6.6: *Responses and noise attenuation of the closed-loop system with different pre-filters and B_0-spline post-filter. The letters in the first column correspond to the letters in Table 6.5. See the text for discussion.*

#	t_r	M_p	t_s	IAE	ISE	ITAE	ITSE	Noise %
a	1.162	4.590	3.681	0.964	0.661	0.672	0.275	1.002
b	1.187	4.590	3.761	0.989	0.680	0.706	0.290	0.771
c	1.230	4.590	3.901	1.036	0.716	0.769	0.320	0.610
d	1.360	4.590	4.314	1.173	0.819	0.968	0.414	0.423
e	1.662	4.590	5.237	1.454	1.024	1.465	0.643	0.241
f	2.324	4.590	7.297	2.012	1.416	2.780	1.234	0.099
z	1.187	4.590	3.752	0.979	0.670	0.695	0.283	0.518

procedure, the value of the overshoot M_p is constant in all cases. Furthermore, we see that the response of the FOL filters becomes worse when the filters' cut-off frequency ω_f reduces. The B_0-spline has a response which is very close to that of the FOL filter with $\omega_s/\omega_f = \pi$. This also follows from the step responses, which are not included here.

Values for noise suppression are given in the last column of Table 6.6. The quantity shown is the relative noise variance of the plant's output *y*, defined by:

$$\frac{\mathrm{Var}\, y}{\mathrm{Var}\, n} \times 100\%,$$

where *n* is the noise signal which is added to the feedback path. All numbers are averages taken over 20 experiments. We see that, for the FOL filters, the noise suppression becomes better as the cut-off frequency reduces. This is in agreement with the suppression values of Table 6.5. The noise suppression of the ZOH is better than that of the FOL filter with $\omega_f = \omega_s/\pi$ (b).

6.5 Evaluation

In this chapter we have studied the effects of selecting pre-filters and post-filters in a closed-loop control system. We analyzed the Multirate Sampled Data System in the Z-domain. Some general conclusions on the analysis of the $K(z)$ transfer functions and the simulations with different filters are stated below:

- The analysis of $K(z)$ was carried out for a simple second-order system. The calculations are quite lengthy, and will be difficult to carry out for more complex systems and higher down-sampling factors. A strong estimation of system stability can be obtained by studying the stability of $K(z)$. The different filter combinations increase the complexity of $K(z)$ compared to the standard case of no pre-filter and ZOH reconstruction.

- From the experiments with different filter combinations we conclude that the filter length is the most dominant parameter. Any attempts to obtain a better signal reconstruction do not result in better system performance, due to the increased phase lag of the longer filters involved.

- If an anti-alias filter is required anyway, the situation is different. In this case a B_0-spline pre-filter gives an overall response which is similar to the response corresponding to the FOL filter with $\omega_s/\omega_f = \pi$. This response is quite satisfactory. The noise suppression is better than that of the FOL $(\omega_s/\omega_f = \pi)$, which is, according to [CCP73], satisfactory. We conclude that the B_0-spline is a good compromise between response and noise suppression. Since the filter *requires no further tuning*, i.e., the filter characteristics are completely determined by the sampling frequency, it is an interesting alternative in control applications.

- From experiments with some other first- and second-order plants, we can draw the same conclusions. We believe that the conclusions regarding the effects of extra filters and comparison between B_0-spline and FOL filter remain valid for a general plant. However, we cannot state that a certain filter yields sufficient suppression of aliasing effects in the general case. This has to be verified for each plant individually.

Using similar arguments as in Section 5.2 we assume that the conclusions drawn for the MSDS system also hold for the SDS system of Figure 6.3.

Finally, we return to the questions raised in Section 6.1. We conclude that, in a noiseless environment, the overall system behavior is negatively affected by inserting a pre-filter and/or replacing the ZOH by a more complex reconstruction method. The most apparent parameter is the phase lag which is longer for more complex filters. The L^2-optimal combination of B_0-spline pre- and post-filter has a response similar to other filter combinations with the same lag. If dealing with a noisy environment, pre-filtering may be required to reduce the effects of aliasing. In this case, a B_0-spline turned out to be a good alternative. The filters must be taken care of in the design procedure.